Journal of Marine Science and Technology

Volume 21 | Issue 4 Article 11

MODEL SIMULATION OF ASIAN DUST AND IRON DEPOSITIONS OVER THE EAST ASIAN MARGINAL SEAS

Fujung Tsai
Department of Marine Environmental Informatics, National Taiwan Ocean University, Keelung, Taiwan, R.O.C,
fujung@mail.ntou.edu.tw

Recommended Citation
Tsai, Fujung (2013) "MODEL SIMULATION OF ASIAN DUST AND IRON DEPOSITIONS OVER THE EAST ASIAN MARGINAL SEAS," *Journal of Marine Science and Technology*: Vol. 21: Iss. 4, Article 11.
DOI: 10.6119/JMST-013-0501-1
Available at: https://jmstt.ntou.edu.tw/journal/vol21/iss4/11

MODEL SIMULATION OF ASIAN DUST AND IRON DEPOSITIONS OVER THE EAST ASIAN MARGINAL SEAS

Acknowledgements

I extend my gratitude to Dr. Shih-Chieh Hsu for providing the dry and wet deposition fluxes of dissolved Ca in dust particles, and to Taiwan's Environmental Protection Agency for providing the PM10 and rainfall data from their website. I likewise extend my gratitude to Cheng-Han He and Jia-ling Wen for their assistance in preparing the data. This study is supported by NSC 98-2611-M-019-019-MY3 project.

Journal of Marine Science and Technology, Vol. 21, No. 4, pp. 460-468 (2013)
DOI: 10.6119/JMST-013-0501-1

MODEL SIMULATION OF ASIAN DUST AND IRON DEPOSITIONS OVER THE EAST ASIAN MARGINAL SEAS

Fujung Tsai

Key words: Asian dust, TAQM, dry and wet deposition, iron.

ABSTRACT

This study applies a dust model to investigate Asian dust and iron depositions on the East Asian marginal sea during the months of the northeasterly monsoon from November to May, when dust events are often observed. Simulated dry and wet depositions of dust are compared with measurements obtained from Taipei, Taiwan. According to the model simulation, higher concentrations of atmospheric dust occur from March to May over East Asia, resulting in greater dry and wet deposition fluxes of dust and iron within these months than other months. The monthly averaged dry and wet deposition fluxes of iron are 0.6 and 0.7 mg m^{-2} day^{-1}, respectively, over the East China Sea, and are five to six times lower over the South China Sea. The wet depositions of dust and iron demonstrate sporadic distributions over the marginal sea, rather than decreasing with downwind distance as occurs with dry deposition.

I. INTRODUCTION

The atmosphere is one of the important process that carries nutrients to the ocean. The terrigenous material transported by aerosol particles can affect the marine ecology and sea surface chemistry [2, 6, 10, 17, 27]. Aerosol particles that contain nitrogen, phosphorus, silicon, and iron are important phytoplankton nutrients. Among these nutrients, iron has raised the most concern in recent decades [4, 24]. Atmospheric iron is mainly contributed by dust particles [23]. In East Asia, the Taklamakan and Gobi Deserts and the Loess Plateau in China are the main sources of dust (Fig. 1). From late October to early May, when a frontal passage occurs over these deserts, the strong surface winds associated with the unstable air is favorable for dust generation. During the northeasterly monsoon, dust particles are carried downwind toward the East Asian marginal sea, such as the East and South China Seas, providing iron nutrients via the dry and wet depositions of dust particles [12].

Among the iron species in dust particles, soluble iron is the species that can be uptake by phytoplankton and supports the nitrogen fixation of some organisms [25]. The deposition of soluble iron into the ocean has been shown to enhance phytoplankton blooms over open oceans of high nutrient low chlorophyll [4]. Phytoplankton enhancement potentially leads to atmospheric cooling through the absorption of atmospheric carbon dioxide [18]. In addition to the impact from phytoplankton, the excretion of dimethyl sulfide (DMS) through the biological role of phytoplankton has both direct and indirect impacts on climate change. DMS is an important source of atmospheric sulfides, which can directly affect the climate through scattering of solar radiation and indirectly through altering cloud microphysics. Both processes have a potential feedback to the global environment [5, 15, 20, 29, 30].

Although the atmosphere is important in supplying iron nutrients to the ocean, few studies assess the atmospheric deposition of iron over East Asia, and among these studies, large variations of iron deposition are found [12]. For example, the annual deposition rate of iron over the North Pacific observed by Duce and Tindale [6] is 17 g yr^{-1}, but estimates by Jickells and Spokes [19] and Gao *et al*. [9] are less than half and less than one-fifth of the Duce and Tindale's estimates, respectively. Studies of iron deposition over the East Asian marginal sea are even more scarce and rely on limited in situ measurements or measurements from short-term cruises [12, 14]. The estimate of atmospheric deposition of iron is then calculated through multiplying the atmospheric concentration by the estimated settling velocity or scavenging rate. These deposition rates may not be applicable to a variety of weather conditions or entire marine areas. Therefore, a more thorough calculation of dust deposition over the whole domain and a longer period are essential.

To understand the dust and iron deposition on the East Asian marginal sea over a longer time period, this study simulates the dust and iron deposition by using a three-dimensional (3-D) dust model and compares the results with observations

Paper submitted 01/29/13; revised 04/12/13; accepted 05/01/13. *Author for correspondence: Fujung Tsai (e-mail: fujung@mail.ntou.edu.tw).*
Department of Marine Environmental Informatics, National Taiwan Ocean University, Keelung, Taiwan, R.O.C.

obtained in Taiwan. First, the calculated dust concentrations and depositions are compared with the observations. Then, simulated atmospheric dust concentration and dry and wet depositions of dust as well as iron, over the marginal sea (including East and South China Seas) are quantified during the northeasterly monsoon when Asian dust is carried downwind to these areas.

II. METHODOLOGY

1. Sampling

Dust depositions are sampled by total deposition and wet deposition buckets on the rooftop of the Institute of Earth Sciences at Academia Sinica (121.61°E, 25.04°N) in Taipei, Taiwan in 2008 (Fig. 1). Total deposition sampling includes both dry and wet depositions. Dry deposition is calculated by subtracting wet deposition from the total deposition. Depositions are sampled either weekly or once every two days. Sampling results are divided into soluble and insoluble portions. The soluble ions of dust contains elements such as K^+, Mg^{2+}, and Ca^{2+}. Most metal in dust, such as Al and Fe, is insoluble or has small solubility [14].

Soluble major metal ions are analyzed by using a Perkin Elmer model Elan 6100 quadrupole-based inductively coupled plasma mass spectrophotometer (ICP-MS). The detailed procedures can be found in Hsu *et al*. [13]. As Ca^{2+} is highly soluble with a relatively small variability compared to other soluble species in dust particles, its dissolved concentration is used for comparison with the model results. To compare the Ca^{2+} deposition flux between the model simulation and the samplings, the simulated Ca^{2+} is assumed to account for 8% of the dust mass and to have 80% solubility, based on previous studies [14, 35]. The simulated deposition flux of dissolved Ca^{2+} is calculated by multiplying the dust concentrations with the Ca^{2+} fraction and its solubility.

To compare the model results with the samples, the observed hourly PM_{10} (particulate matter, less than 10 μm in diameter) concentration and rainfall amount, respectively, are also provided. The observed PM_{10} concentration is obtained from the Wanli Station, located at the northern tip of Taiwan, and 35 km from the Ca^{2+} sampling site. Wanli is a small town facing the seashore of northern Taiwan, so the measurement obtained from this station is often used to represent the influence of Asian outflow on Taiwan [21, 26]. The good correlation between the Ca^{2+} sampling and the PM_{10} concentration indicates the arrival of the dust event. The correlation is presumably better than any other station, since the PM_{10} concentration at other station could be contaminated by local pollutants. The rainfall amount is obtained from the Hsichih Station, located about 8 km from the Ca^{2+} sampling site, because the station is the closest station to the sampling site with rainfall measurement available. For those periods with insufficient wet deposition measurement, the model simulated wet deposition can be verified through dry deposition measurement before and after the period and the rainfall amount of the period obtained from Hsichih Station. Both Wanli and Hsichih stations are maintained by Taiwan's Environmental Protection Administration (EPA).

2. Model Descriptions

The Taiwan Air Quality Model, which includes a dust module, (TAQM-Dust) is applied to simulate the regional dust distributions over East Asia [34]. The original TAQM is a 3-D regional model used to simulate the distribution of trace gases and particles [16]. The model domain covers East Asia from about 10°N to 60°N and 70°E to 150°E (Fig. 1), with a horizontal resolution of 81 km × 81 km. Vertically, the model is divided into 15 sigma levels, with a higher vertical resolution ranging from roughly 40 m near the surface to 1 km to 2 km near the tropopause of 100 hPa. A dust simulation is produced for the months of northeasterly monsoon, that is, from January to May and November to December, in 2008 and compared with observations. The initial model domain contains no dust concentration. It takes at least one week to generate dust concentration in the model domain. To minimize the influence of the initial conditions on model simulations, the first month of the model simulation (i.e., January 2008) is not included in the discussion.

The meteorological data, such as wind, temperature, and pressure, for dust transport in the model is obtained from National Center for Atmospheric Research (NCAR)/Penn State Mesoscale Meteorological Model (MM5) [1, 7, 11] simulations. Initial and boundary input for MM5 include the Tropical Ocean and Global Atmosphere (TOGA) advanced analysis obtained from the European Center for Medium-Range Weather Forecast (ECWMF). For each day of 2008, MM5 is run for two days, but only the second day of simulation is used for connecting the data into the whole year for used in CMAQ. The first day of MM5 simulation is not used to avoid the initial problem of the model. To ensure the meteorological fields are well simulated, the four-dimensional data assimilation scheme is selected in the model based on the ECWMF TOGA advanced analysis data. The analysis data with surface and upper air analyses are archived on a 1.125 × 1.125 degree grid with a six-hour interval.

TAQM-Dust consists of dust emission, transport, and deposition modules. In the dust emission module, developed based on Wang *et al*. [35], dust particles are divided into 12 size bins ranging from 0.13 μm to 20.13 μm. Dust transport is computed using Bott's [3] scheme, which can minimize the numerical diffusion problem. Horizontal and vertical advection and diffusion are included in the dust transport module, as well as a boundary layer mixing scheme from Pleim and Chang [28], so the chemical species can be rapidly transported upward through the troposphere under convective conditions. Wet deposition of dust is calculated using a diagnostic cloud module **[**36]. The subcloud removal of dust particles is considered in the wet removal process. Dry deposition of dust is calculated from the deposition velocities and the dust concentration in the model surface layer. Dry deposition velocities are de rived

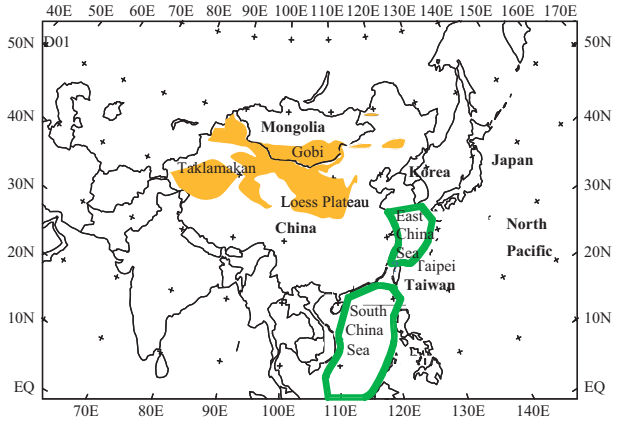

Fig. 1. Map of East Asia, deserts in China (yellow shaded area), East and South China Seas (green circle), and the sampling site at Taipei (star), Taiwan.

from the aerodynamic, sub-layer and canopy resistances [30]. Gravitational settling of dust particles above the surface layer is also included among the dry deposition processes.

III. RESULTS

Fig. 2 shows the measured Ca^{2+} deposition flux and the PM_{10} concentrations obtained respectively from the Taipei and Wanli stations in Taiwan during spring 2008, along with a comparison against simulated deposition fluxes. The dry deposition of Ca^{2+} in dust particles are enhanced in four episodic dust events during 2008, namely the events from February 27 to March 10, March 24 to 28, April 23 to 28, May 13 to 23 (including May 13 to 18 and May 20 to 23), peaking close to 10 mg m^{-2} day^{-1} on April 23. The high dry deposition flux of Ca^{2+} is consistent with high PM_{10} concentrations measured at the Wanli Station. Since the Wanli Station, located at the northern tip of Taiwan, often receives aerosols from Asian outflow in spring [22] and Ca^{2+} predominantly originates from dust particles [14], this consistency indicates that Asian dust activities contribute to the enhanced dry deposition flux of Ca^{2+} in Taipei.

For the four major dust events with observed Ca^{2+} deposition flux of at least 4 mg m^{-2} day^{-1} discussed above, the simulated dry deposition fluxes reached similar magnitude during the same episodic dust events, and reasonably captures the dust events when comparing with observed PM_{10} concentrations (Fig. 2). However, the simulated magnitude and timing of dry deposition flux of Ca^{2+} slightly differ from the measurement. Several factors can contribute to this discrepancy. First, anthropogenic pollution is also a source of Ca^{2+}, though the contribution is estimated to be only around 5% on average [23]. If anthropogenic Ca^{2+} is sampled, the sampled concentrations will be different from the simulated concentrations of Ca^{2+} calculated from dust concentrations alone. Second, the Ca^{2+} mass fraction in dust particles and its dissolution percentage vary by a magnitude of two depending on the source

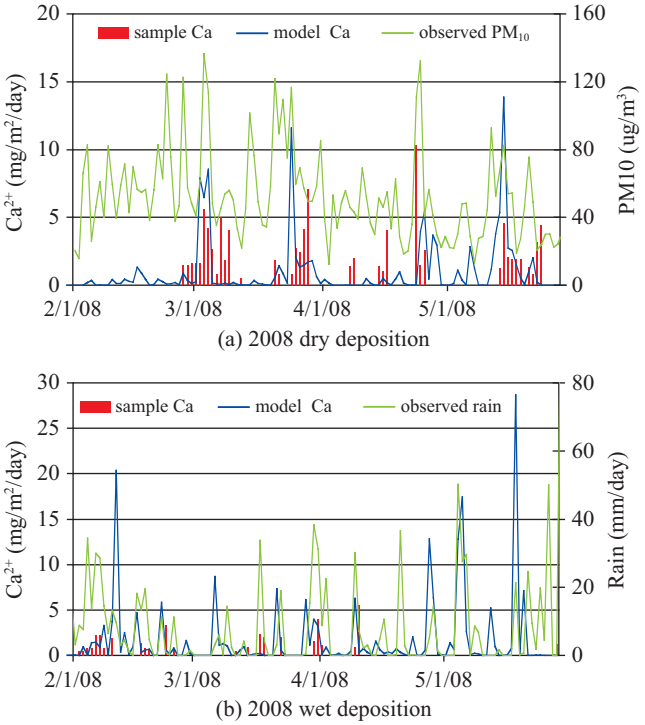

Fig. 2. The sampled and modeled (a) dry and (b) wet deposition flux of Ca^{2+} (mg m^{-2} day^{-1}) in dust particles at Taipei, Taiwan from February to May 2008. Observed PM_{10} concentrations (μg m^{-3}) and rainfall amount (mm/day) are included in the dry and wet deposition plots, respectively.

location of dust and the dissolution condition. These variations can contribute to the discrepancy when comparing against the model simulation, which applies an average value obtained from previous measurements [14, 36]. Moreover, the model resolution can contribute to the discrepancy if dust is not homogeneously distributed over the model domain. Both the meteorological and chemical simulation can also have some biases and were discussed in previous studies [20, 35]. Therefore, the comparison of deposition flux between the model and measurements is more challenging than the comparison of dust concentration in the air between them, which has been demonstrated to be consistent in previous studies [34]. Nevertheless, the results demonstrate that the model has well captured the dry deposition of these dust events.

In addition to dry deposition, Fig. 2 also shows the measured wet deposition flux of Ca^{2+} and the rainfall amount at Taipei in spring 2008, compared with the model simulation. The observed wet deposition flux is elevated during February, mid-March, and early April, with a maximum of about 5 mg m^{-2} day^{-1}. Although the model simulation is mostly consistent with measurements during these periods, there is insufficient measurement from late April to May, when Ca^{2+} measurement is not available. To compensate for the insufficient measurement, observed rainfall amount from the nearby EPA station is added for comparison. Fig. 2(b) shows that the calculated wet deposition of Ca^{2+} peaks during some rainfall events

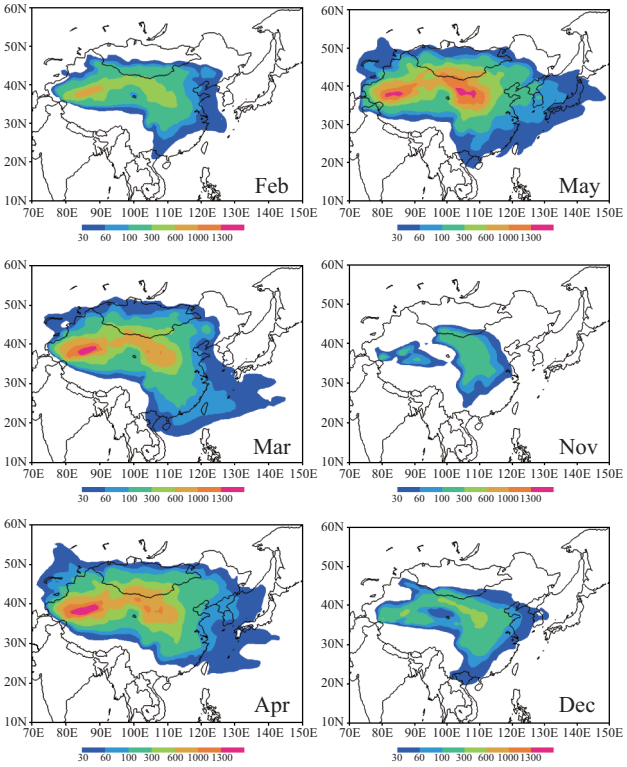

Fig. 3. Monthly averaged dust concentrations (μg m^{-3}) in the air over East Asia during the months of northeasterly monsoon in 2008.

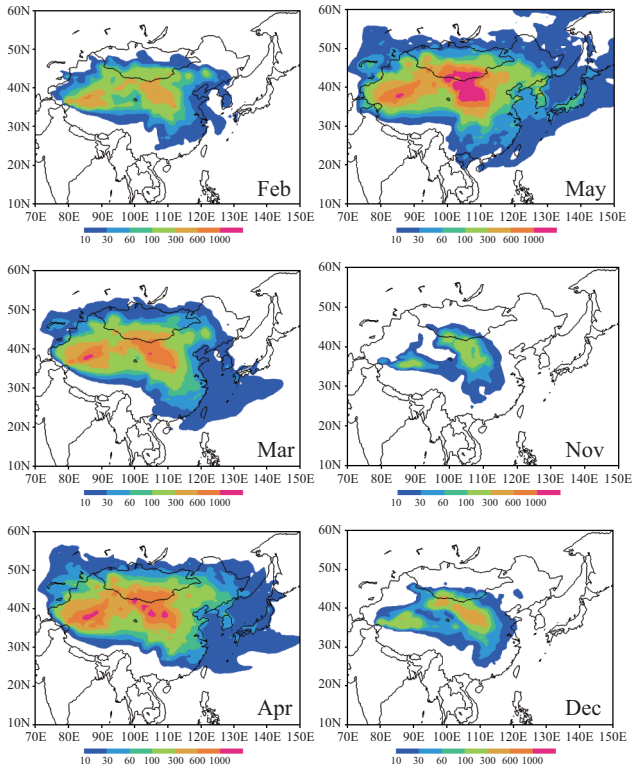

Fig. 4. Monthly averaged dry deposition flux of dust (mg m^{-2} day^{-1}) over East Asia during the months of northeasterly monsoon in 2008.

and reached a maximum of 28 mg m^{-2} day^{-1} on May 19. The simulated maximum wet deposition occurs between the dust events on May 13 to18 and May 20 to 23, within which rainfall is also observed, resulting in an enhanced wet deposition flux of Ca^{2+}. During other period, the wet deposition sometimes peak although rainfall is modest, because wet deposition also strongly depend on dust concentration. The result shows that the calculated wet removal of Ca^{2+} is reasonable when comparing with the observations of rainfall and dust event.

To estimate the impact of Asian dust on the East Asian marginal sea, including the East and South China Seas, the atmospheric dust concentration, and the dry and wet depositions of dust and iron, are simulated during the months of northeasterly monsoon, when Asian dust events are transported downwind. Fig. 3 shows the simulated monthly averaged dust concentration in the air on February-May and November-December 2008. The enhanced dust concentrations are mainly located over the deserts, including the Taklimakan Desert, Gobi Desert and Loess Plateau (also see Fig. 1). Higher concentrations are observed from March to May when dust events are active, similar to results in previously studies [23]. The maximum concentration of these months reaches more than 1300 μg m^{-3}, and decreases to less than 300 μg m^{-3} to 800 μg m^{-3} during the other months. In May, when dust events are active during the year (http://baike.baidu.com/view/3381041.htm), dust concentrations can reach approximately 100 μg m^{-3} over the northeastern coast and the marginal sea of China.

Fig. 4 shows the simulated monthly averaged dry deposition flux of dust over East Asia. The dry deposition flux of dust is calculated from the surface concentrations of dust and deposition velocity, and thus the distribution pattern of the dry deposition flux is somewhat similar to that of the dust concentration. The deposition flux reaches a maximum in May, because of the higher dust concentration than in other months (Fig. 3). The maximum flux of over 1000 mg m^{-2} day^{-1} is calculated over the desert areas in China. During this month, more than 30 mg m^{-2} day^{-1} of deposition flux is also observed over the eastern coast and the marginal sea.

In addition to dry deposition, wet deposition also contributes to dust deposition to the sea surface. The wet deposition of dust is attributed to both precipitation and dust concentration. Although dust is most concentrated over deserts, precipitation occurs more frequently over the coastal regions (Fig. 5). As a result, wet deposition of dust is observed over both the continent and the marginal seas, with a maximum deposition flux of over 300 mg m^{-2} day^{-1} over northern China in May (Fig. 6). The deposition flux reaches approximately 50 mg m^{-2} day^{-1} over the northern marginal sea of East Asia in the same month.

On average, the simulated dry deposition flux of dust is 15 and 2 mg m^{-2} day^{-1} over the East and South China Seas, respectively, during the northeasterly monsoon, slightly lower than the wet deposition flux of dust (18 and 5 mg m^{-2} day^{-1}, respectively). Both the deposition flux over the South China

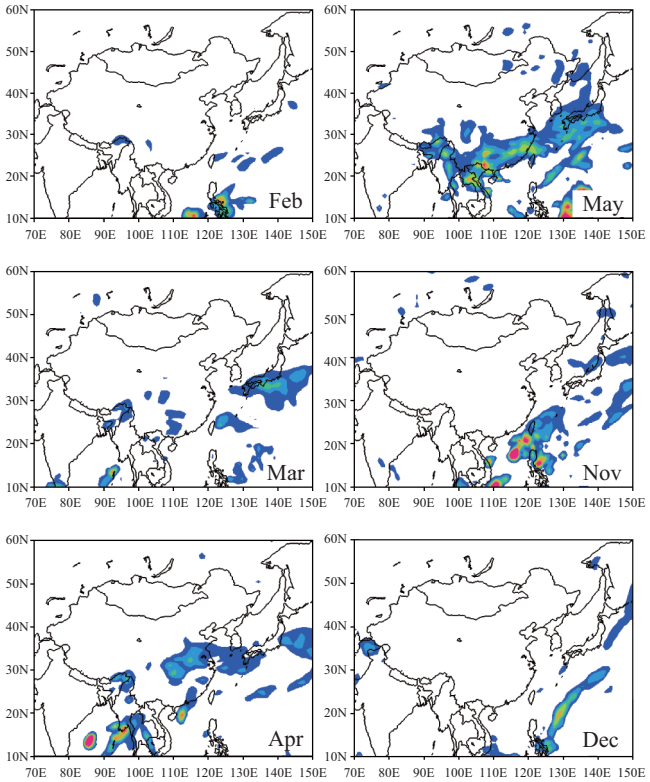

Fig. 5. Monthly averaged rainfall amount (mm) over East Asia during the months of northeasterly monsoon in 2008.

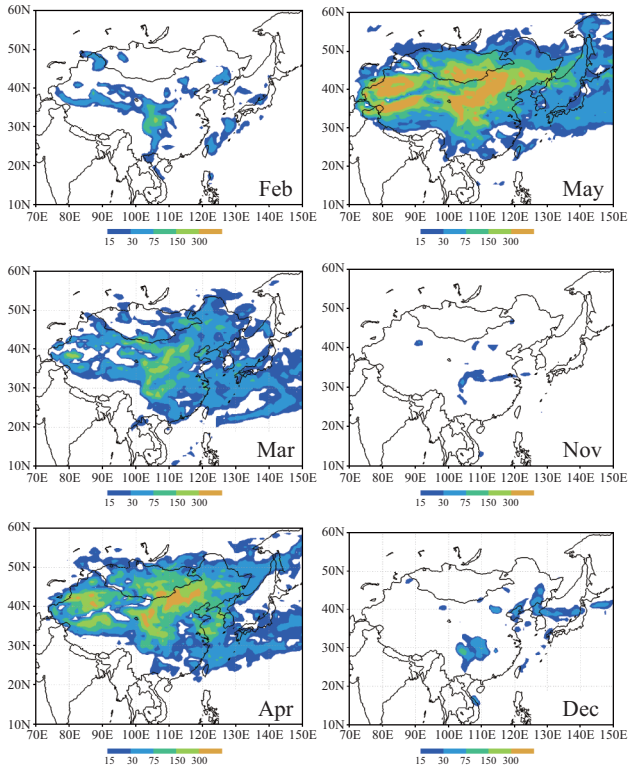

Fig. 6. Monthly averaged wet deposition flux of dust (mg m^{-2} day^{-1}) over East Asia during the months of northeasterly monsoon in 2008.

Sea is 5 to 10 times lower than that in the East China Sea. The averaged dry deposition flux of dust over the East China sea is similar to those extrapolated from measurements by Hsu *et al*. [13], while the simulated wet deposition flux in the current study is lower than in their study (38 mg m^{-2} day^{-1}). On the other hand, Gao *et al*. [9] also estimated an almost equivalent value between the dry and wet deposition fluxes of dust, although their values (about 35 mg m^{-2} day^{-1}) are both greater, because they are measured over the northern East China Sea instead of the entire East China Sea. If the almost equivalent value between the dry and wet deposition fluxes of dust obtained from Gao *et al*. [9] is applied to our studies, the averaged wet deposition flux will be close to the result we obtained. Comparing to these studies, we found that our simulated wet deposition flux is in the reasonable range.

Monthly averaged deposition of iron over the marginal sea, including the East China Sea and South China Sea, is calculated from the dust deposition by assuming that iron accounts for 4% of the mass of dust particles, according to previous measurements [36]. Fig. 7 shows that the simulated dry deposition flux of iron ranges from less than 0.05 mg m^{-2} day^{-1} to 1 mg m^{-2} day^{-1} over East China Sea during the months of the northeasterly monsoon. The maximum flux over the East China Sea occurs in March, when the dry deposition flux is about 1 mg m^{-2} day^{-1}. Since the major dust events of the year occurred in early March and dust was transported southeastward (see dry deposition from Taiwan in Fig. 2(a)), the dry deposition flux of iron peaked in that month. The minimum deposition flux over the East China Sea occurs from November to December, when the flux is mostly below 0.25 mg m^{-2} day^{-1}. For all months, the dry deposition flux decreases with distance away from the continent.

Similarly, the wet deposition of iron over the East China Sea is calculated from the wet deposition of dust. Fig. 8 shows the spatial distribution of the wet deposition flux of iron during the months of the northeasterly monsoon. The wet deposition of iron reaches a maximum in March-April when the dust concentration and precipitation are greater (also see Fig. 2). The maximum wet deposition flux is over 2.5 mg m^{-2} day^{-1} over the East China Sea, which is greater than the maximum value of dry deposition flux (1 mg m^{-2} day^{-1}) over the area. The deposition decreases when precipitation and dust activity is less, and reaches a minimum on November, when the deposition flux is mainly below 0.25 mg m^{-2} day^{-1} over the East China Sea. Unlike its dry deposition, the wet deposition of iron demonstrates an uneven distribution over the East China Sea.

Over the South China Sea, the dry deposition of iron decreases with distance from the Asian continent due to the deposition of dust during southward transport (Fig. 9). The deposition flux reaches a maximum in May, when the flux is mainly greater than 0.05 mg m^{-2} day^{-1} over the northern South China Sea, but decrease rapidly southward to below 0.05 over the southern South China Sea. The minimum deposition flux

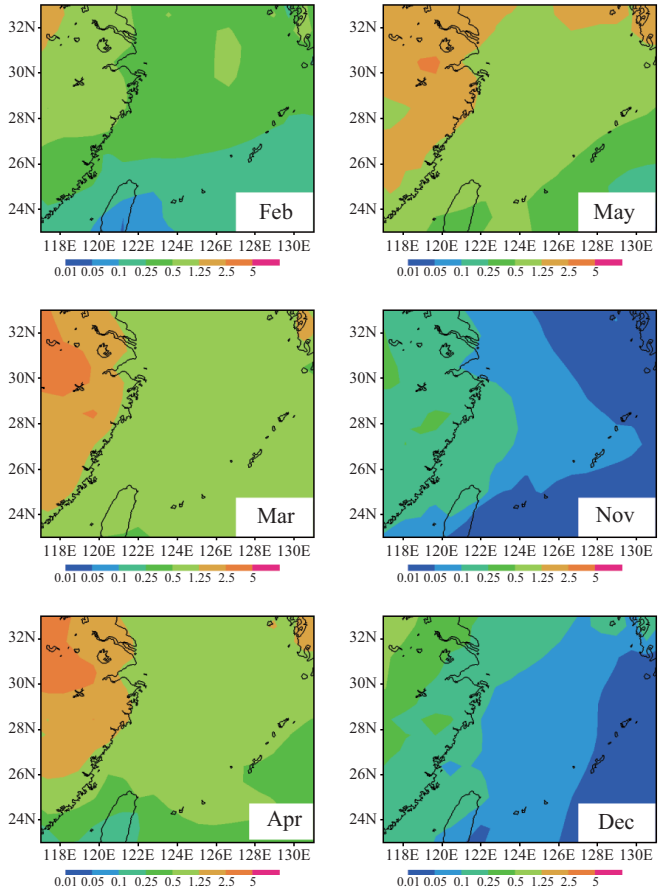

Fig. 7. Monthly averaged dry deposition flux of iron (mg m^{-2} day^{-1}) over East China Sea during the months of northeasterly monsoon in 2008.

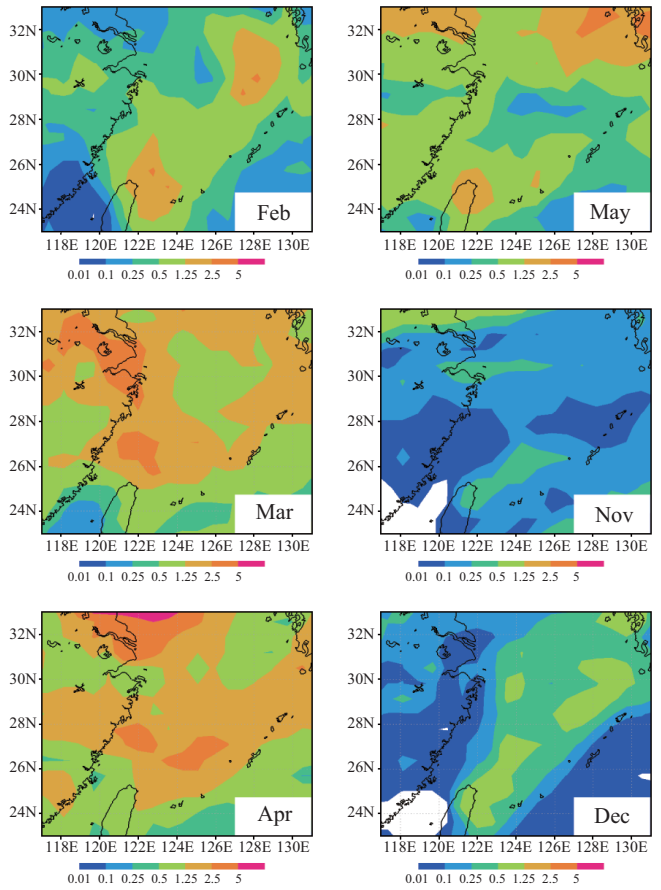

Fig. 8. Monthly averaged wet deposition flux of iron (mg m^{-2} day^{-1}) over East China Sea during the months of northeasterly monsoon in 2008.

occurs in November, when the deposition flux is mainly below 0.1 mg m^{-2} day^{-1} over the whole area.

The wet deposition of iron over the South China Sea is also greater than the dry deposition of iron over the area (Fig. 10). The maximum wet deposition flux occurs in May, when the flux is predominately greater than 0.1 mg m^{-2} day^{-1} over the northern South China Sea. On the other hand, the uneven distribution of the wet deposition flux extends far south to the southern South China Sea in March, primarily because of the southeastward transport of the major dust event in early March.

Simulated dry and wet deposition fluxes of iron over the East and South China Seas are summarized in Fig. 11. Over the East China Sea, the monthly averaged dry deposition flux ranges from less than 0.1 mg m^{-2} day^{-1} in November to 1.1 mg m^{-2} day^{-1} in March (Fig. 11(a)). The wet deposition flux is greater than the dry deposition flux in nearly every month, with values ranging from 0.15 mg m^{-2} day^{-1} in November to 1.4 mg m^{-2} day^{-1} in April. The mean wet deposition flux of iron over the East China Sea, during the northeasterly monsoon season is about 0.7 mg m^{-2} day^{-1}, about 1.2 times greater than the dry deposition flux (0.6 mg m^{-2} day^{-1}). The total deposition flux of iron over the East China Sea is about 1.3 mg m^{-2} day^{-1}. This value is lower than the value (3.1 mg m^{-2} day^{-1}) estimated by Hsu *et al*. averaged from 2002 to 2006 [12], which are also moderate dust activity years. The lower value is attributed to the fraction of Fe (4%) in dust particles assumed in the current study is lower than that in their study (about 5.5%). In addition, the wet deposition flux of dust, and thus iron, calculated in our study is also lower than in their study, as discussed previously.

Both simulated deposition fluxes are lower over the South China Sea due to the decrease in dust concentration during their southward transport (Fig. 11(b)). The dry deposition flux ranges from 0.04 mg m^{-2} day^{-1} in November to 0.2 mg m^{-2} day^{-1} in May over the South China Sea. The mean dry deposition flux of 0.1 mg m^{-2} day^{-1} is only one-sixth of the value over the East China Sea. The wet deposition flux over the South China Sea is slightly larger than that of the dry deposition flux. The mean value of the wet deposition flux of 0.15 mg m^{-2} day^{-1} over the South China Sea is only one-fifth of the value over the East China Sea and the maximum deposition flux of 0.25 mg m^{-2} day^{-1} occurs in March.

IV. CONCLUSION

The TAQM-Dust model, with incorporated dust module is

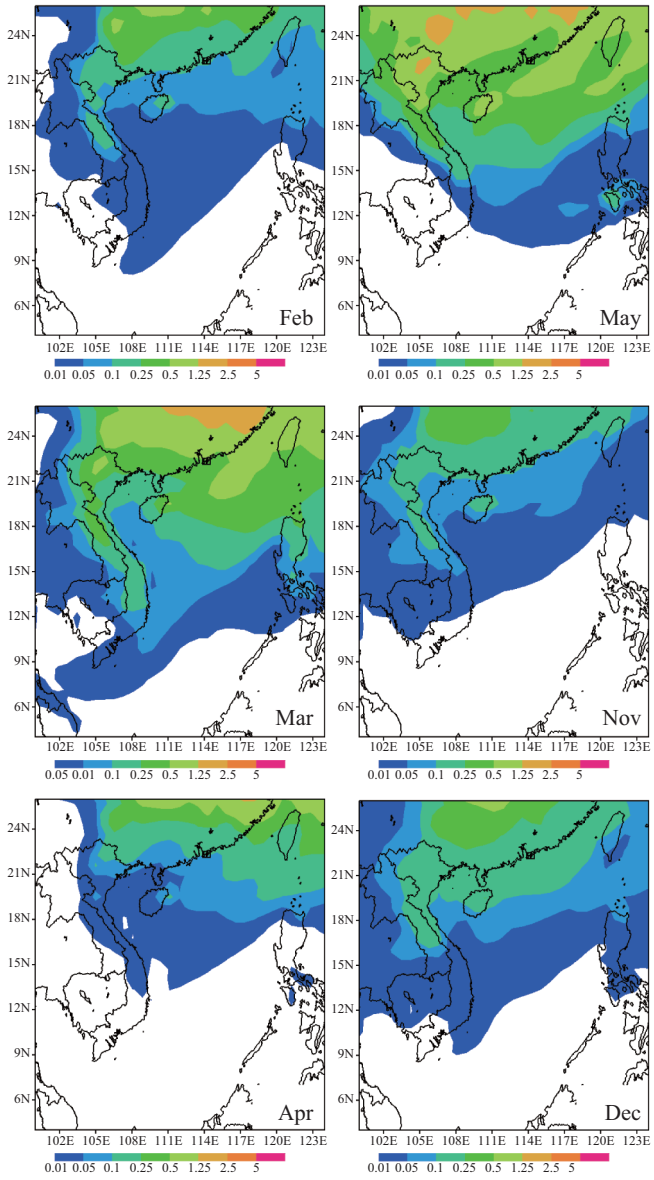

Fig. 9. Monthly averaged dry deposition flux of iron (mg m^{-2} day^{-1}) over South China Sea during the months of northeasterly monsoon in 2008.

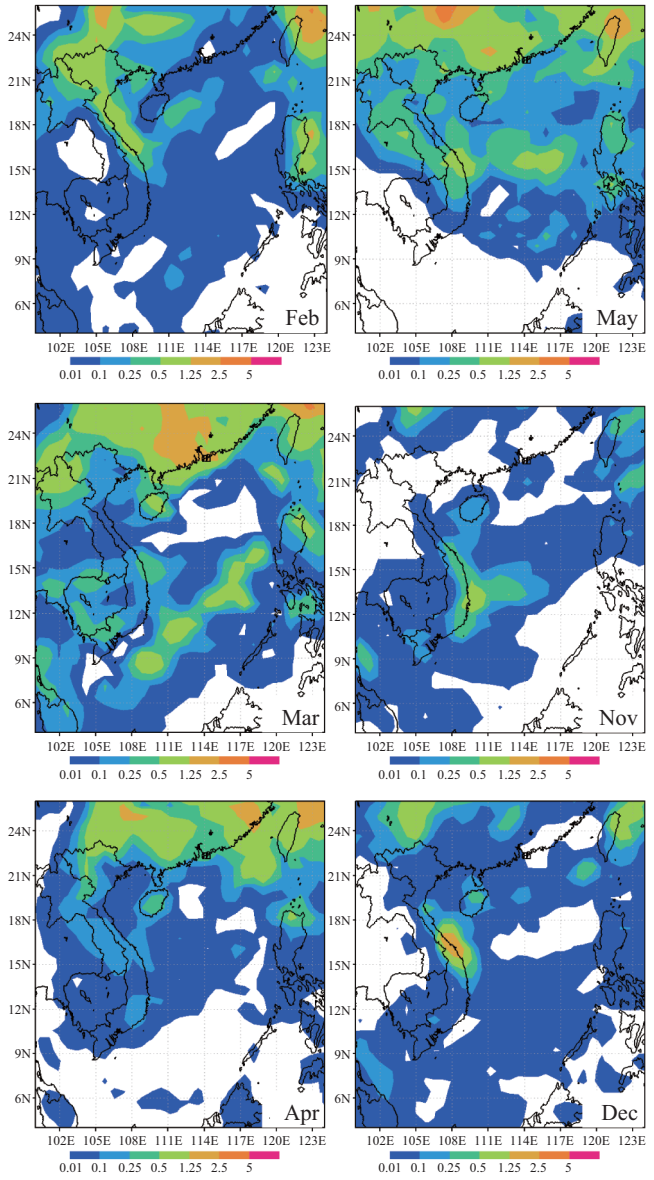

Fig. 10. Monthly averaged wet deposition flux of iron (mg m^{-2} day^{-1}) over South China Sea during the months of northeasterly monsoon in 2008.

applied to investigate dust and iron deposition over the East Asian marginal sea during the months of the northeasterly monsoon, when dust events are often observed. The results of dry and wet deposition of dust are compared with the measurements obtained from Taipei, Taiwan. The comparison of dissolved Ca^{2+} concentrations from the dry and wet depositions of dust particles demonstrates that the model results are fairly reasonable in 2008 when measurements are available. The dry and wet depositions of dust and iron are then calculated over the East Asian marginal sea, including the East China Sea and the South China Sea.

The results demonstrate that high concentrations of dust in the air are observed from March to May, resulting in high dry and wet deposition fluxes of dust and iron calculated within these months over the East Asian marginal sea. The dry depositions of dust and iron are concentrated over the deserts of China, and decrease with distance downwind from the continent. In comparison, the wet deposition of dust and iron shows an uneven distribution over East Asia and the marginal sea due to the combined contributions from precipitation and dust concentration.

By assuming that iron accounts for 4% of mass in dust particle, model results suggest that the averaged dry deposition of dust is about 15 mg m^{-2} day^{-1}, while the averaged wet deposition flux of dust is about 18 mg m^{-2} day^{-1} over the East China Sea. For iron, the averaged dry and wet deposition flux are 0.6 mg m^{-2} day^{-1} and 0.7 mg m^{-2} day^{-1}, respectively, over East China Sea. Both deposition fluxes over South China Sea

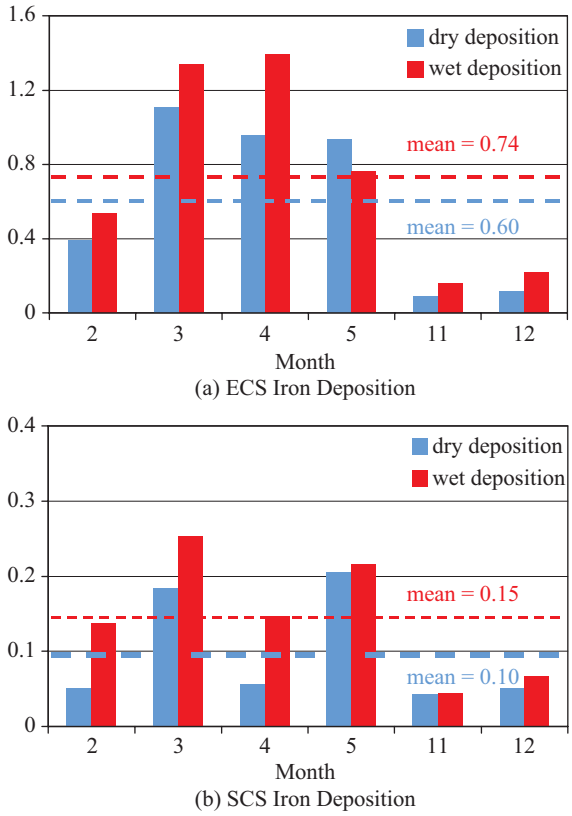

Fig. 11. Monthly averaged dry and wet depositions flux of iron over (a) East China Sea and (b) South China Sea.

are five to six times lower than those over the East China Sea due to the distance away from the source area, and are only about 0.1 mg m^{-2} day^{-1} and 0.15 mg m^{-2} day^{-1} on average during the months of the northeasterly monsoon respectively.

In this study, the impact of Asian dust deposition over the marginal sea of East Asia in 2008 is simulated. The results represent the dust effects in a regular year, when dust activity is moderate. The deposition of iron and other crustal nutrients of dust particle are important to marine biogeochemistry in the East Asian marginal sea. The results of these deposition impacts require further assessment.

ACKNOWLEDGMENTS

I extend my gratitude to Dr. Shih-Chieh Hsu for providing the dry and wet deposition fluxes of dissolved Ca in dust particles, and to Taiwan's Environmental Protection Agency for providing the PM_{10} and rainfall data from their website. I likewise extend my gratitude to Cheng-Han He and Jia-ling Wen for their assistance in preparing the data. This study is supported by NSC 98-2611-M-019-019-MY3 project.

REFERENCES

1. Anthes, R. A. and Warner, T. T., "Development of hydrodynamic models suitable for air pollution and other mesometeorological studies," *Monthly Weather Review*, Vol. 106, pp. 1045-1078 (1978).
2. Arimoto, R., Duce, R. A., Ray, B. J., and Tomza, U., "Dry deposition of trace elements to the western North Atlantic," *Global Biogeochemical Cycles*, Vol. 17, p. 1010 (2003).
3. Bott, A., "A positive definite advection scheme obtained by nonlinear renormalization of the advective fluxes," *Monthly Weather Review*, Vol. 117, pp. 1006-1015 (1989).
4. Boyd, P. W., *et al*., "A mesoscale phytoplankton bloom in the polar Southern Ocean stimulated by iron fertilization," *Nature*, Vol. 407, pp. 695-702 (2000).
5. Charlson, R. J., Schwartz, S. E., Hales, J. M., Cess, R. D., Coakley, J. A., Hansen, J. E., and Hofmann, D. J., "Climate forcing by anthropogenic aerosols," *Science*, Vol. 255, pp. 423-430 (1992).
6. Duce, R. A. and Tindale, N. W., "Atmospheric transport of iron and its deposition in the ocean," *Limnology and Oceanography*, Vol. 36, No. 8, pp. 1715-1726 (1991).
7. Dudhia, J., "A nonhydrostatic version of the Penn State/NCAR mesoscale model: Validation tests and simulation of an Atlantic cyclone and cold front," *Monthy Weather Review*, Vol. 121, pp. 1493-1513 (1993).
8. Gao, Y., Arimoto, R., Duce, R. A., Zhang, X. Y., Zhang, G. Y., An, Z. S., Chen, L. Q., Zhou, M. Y., and Gu, D. Y., "Temporal and spatial distributions of dust and its deposition to the China Sea," *Tellus*, Series B, Vol. 49, pp. 172-189 (1997).
9. Gao, Y., Kaufman, Y. J., Tanre, D., Kolber, D., and Falkowski, P. G., "Seasonal distributions of aeolian iron fluxes to the global ocean," *Geophysical Research Letters*, Vol. 28, No. 1, pp. 29-32 (2001).
10. Greaves, M. J., Elderfield, H., and Sholkovitz, E. R., "Aeolian sources of rare earth elements to the Western Pacific Ocean," *Marine Chemistry*, Vol. 68, pp. 31-38 (1999).
11. Grell, G. A., Dudhia, J., and Stauffer, D. R., "A description of the fifth generation Penn State/MCAR mesoscale model (MM5)," *Technical Note NCAR/TN-398+STR*, National Center for Atmospheric Research, Boulder, Colorado, p. 117 (1994).
12. Hsu, S. C., Liu, S. C., Arimoto, R., Liu, T. H., Huang, Y. T., Tsai, F., Lin, F. J., and Kao, S. J., "Dust deposition to the East China Sea and its biogeochemical implications," *Journal of Geophysical Research*, Vol. 114, D15304, DOI: 10.1029/2008JD011223 (2009).
13. Hsu, S. C., Liu, S. C., Kao, S. J., Jeng, W. L., Huang, Y. T., Tseng, C. M., Tsai, F., Tu, J. Y., and Yang, Y., "Water soluble species in the marine aerosol from the northern South China Sea: High chloride depletion related to air pollution," *Journal of Geophysical Research*, Vol. 112, DOI: 10.1029/2007JD008844 (2007).
14. Hsu, S. C., Wong, G. T. F., Gong, G.-C., Shiah, F.-K., Huang, Y.-T., Kao, S.-J., Tsai, F., Lung, S.-C. C., Lin, F.-J., Lin, I.-I., Hung, C.-C., and Tseng, C.-M., "Sources, solubility, and dry deposition of aerosol trace elements over the East China Sea," *Marine Chemistry*, Vol. 120, pp. 116-127, DOI: 10.1016/j.marchem.2008.10.003 (2010).
15. Huebert, B. J., Bates, T., Russell, P. B., Shi, G. Y., Kim, Y. J., Kawamura, K., Carmichael, G., and Nakajima, T., "An overview of ACE-Asia: Strategies for quantifying the relationships between Asian aerosols and their climatic impacts," *Journal of Geophysical Research*, Vol. 108, No. D23, 8633, DOI: 10.1029/2003JD003550 (2003).
16. Jeng, F.-T., Chang, J. S., Chang, K.-H., Huang, H., and Liu, T., "Taiwan air quality model user manual" Graduate Institute of Environmental Engineering, National Taiwan University, Taipei, Taiwan (2000). (in Chinese)
17. Jickells, T. D., "Atmospheric inputs of metals and nutrients to the oceans - their magnitude and effects," *Marine Chemistry*, Vol. 48, pp. 199-214 (1995).
18. Jickells, T. D., An, Z. S., Andersen, K. K., Baker, A. R., Bergametti, G., Brooks, N., Cao, J. J., Boyd, P. W., Duce, R. A., Hunter, K. A., Kawahata, H., Kubilay, N., laRoche, J., Liss, P. S., Mahowald, N., Prospero, J. M., Ridgwell, A. J., Tegen, I., and Torres, R., "Global iron connections between desert dust, ocean biogeochemistry and climate," *Science*, Vol. 308, pp. 67-71 (2005).
19. Jickells, T. D. and Spokes, L. J., "Atmospheric iron inputs to the ocean,"

in: Turner, D. and Hunter, K. A. (Eds.), *Biogeochernistry of Iron in Seawater*, John Wiley & Sons (2000).
20. Jones, M. S., Brian, A. C., and Jeffrey, S. T., "Evaluation of a mesoscale short-range ensemble forecast system over the northeast United States," *Weather Forecasting*, Vol. 22, pp. 36-55 (2007).
21. Kaufman, Y. J., Tanre, D., and Boucher, O., "A satellite view of aerosols in the climate system," *Nature*, Vol. 419, pp. 215-223 (2002).
22. Liu, C.-M., Young, C.-Y., and Lee, Y.-C., "Influence of Asian dust storms on air quality in Taiwan," *Science of The Total Environment*, Vol. 368, Nos. 2-3, pp. 884-897, DOI: 10.1016/j.scitotenv.2006.03.039 (2006).
23. Liu, T. H., Tsai, F., Hsu, S. C., Hsu, C. W., Shiu, C. J., Chen, W. N., and Tu, J. Y., "Southeastward transport of Asian dust: Source, transport and its contributions to Taiwan," *Atmospheric Environment*, Vol. 43, pp. 458-467, DOI: 10.1016/j.atmosenv.2008.07.066 (2009).
24. Mahowald, N. M., Engelstaedter, S., Luo, C., Sealy, A., Artaxo, P., Nelson, C. B., Bonnet, S., Chen, Y., Chuang, P. Y., Cohen, D. D., Dulac, F., Herut, B., Johansen, A. M., Kubilay, N., Losno, R., Maenhaut, W., Paytan, A., Prospero, J. M., Shank, L. M., and Siefert, R. L., "Atmospheric iron deposition: global distribution, variability, and human perturbations," *Annual Review of Marine Science*, Vol. 1, pp. 245-278 (2009).
25. Martin, J. H. and Fitzwater, S. E., "Iron deficiency limits phytoplankton growth in the North-East Pacific Subarctic," *Nature*, Vol. 331, pp. 341-343 (1988).
26. Mills, M. M., Ridame, C., Davey, M., La Roche, J., and Geider, R. J., "Iron and phosphorus co-limit nitrogen fixation in the eastern tropical North Atlantic," *Nature*, Vol. 429, pp. 292-294 (2004).
27. Ou-Yang, C.-F., Hsieh, H.-C., Wang, S.-H., Lin, N.-H., Lee, C.-T., Sheu, G.-R., and Wang, J.-L., "Influence of Asian continental outflow on the regional background ozone level in northern South China Sea," *Atmospheric Environment*, DOI: 10.1016/j.atmosenv.2012.07.040 (2012).
28. Patterson, C. C. and Settle, D. M., "Review of data on aeolian fluxes of industrial and natural lead to the land and seas in remote regions on a global scale," *Marine Chemistry*, Vol. 22, pp. 137-162 (1987).
29. Pleim, J. and Chang, J. S., "A non-local closure model for vertical mixing in the convective boundary layer," *Atmospheric Environment*, Vol. 26, pp. 965-981 (1992).
30. Ramanathan, V., Crutzen, P. J., Kiehl, J. T., and Rosenfeld, D., "Atmosphere - aerosols, climate, and the hydrological cycle," *Science*, Vol. 294, pp. 2119-2124 (2001).
31. Seinfeld, J. H. and Pandis, S. N., *Atmospheric Chemistry and Physics: From Air Pollution to Climate Change*, 1st Edition, Wiley-Interscience Publisher (1997).
32. Sokolik, I. N. and Toon, O. B., "Direct radiative forcing by anthropogenic airborne mineral aerosols," *Nature*, Vol. 381, pp. 681-683 (1996).
33. Tsai, F., Chen, G. T.-J., Liu, T.-H., Lin, W.-D., and Tu, J.-Y., "Characterizing the transport pathways of Asian dust," *Journal of Geophysical Research*, Vol. 113, D17311, DOI: 10.1029/2007JD009674 (2008).
34. Tsai, F., Liu, T.-H., Liu, S. C., Chen, T.-Y., Anderson, T. L., and Masonis, S. J., "Model simulation and analysis of coarse and fine particle distributions during ACE-Asia," *Journal of Geophysical Research*, Vol. 109, DOI: 10.1029/2003JD003665 (2004).
35. Vautard, R., Beekmann, M., Bessagnet, B., Blond, N., Hodzic, A., Honoré, C., Malherbe, L., Menut, L., Rouil, L., and Roux, J., "The use of MM5 for operational ozone/NO_x/aerosols prediction in Europe: strengths and weaknesses of MM5," *MM5 Workshop*, Boulder, Colo, USA, pp. 1-4 (2004).
36. Walcek, C. J. and Taylor, G. R., "A theoretical method for computing vertical distribution of acidity and sulfate production within growing cumulus clouds," *Journal of Atmospheric Science*, Vol. 43, pp. 339-355 (1986).
37. Wang, Z., Ueda, H., and Huang, M., "A deflation module for use in modeling long-range transport of yellow sand over East Asia," *Journal of Geophysical Research*, Vol. 105, pp. 26947-26959 (2000).
38. Zhang, X. Y., Gong, S. L., Shen, Z. X., Mei, F. M., Xi, X. X., Liu, L. C., Zhou, Z. J., Wang, D., Wang, Y. Q., and Cheng, Y., "Characterization of soil dust aerosol in China and its transport and distribution during 2001 ACE-Asia: 1. Network observations," *Journal of Geophysical Research*, Vol. 108, No. D9, 4261, DOI: 10.1029/2002JD002632 (2003).